

See discussions, stats, and author profiles for this publication at: <https://www.researchgate.net/publication/220020794>

# Infrared Investigation of Fluoride Occluded in Double Four-Member Rings in Zeolites

ARTICLE *in* THE JOURNAL OF PHYSICAL CHEMISTRY B · MARCH 2002

Impact Factor: 3.3 · DOI: 10.1021/jp013190o

---

CITATIONS

16

---

READS

13

4 AUTHORS, INCLUDING:



**Francisco Manuel Marquez**

Universidad del Turabo

**127** PUBLICATIONS **1,568** CITATIONS

SEE PROFILE



**Miguel Cambor**

Spanish National Research Council

**131** PUBLICATIONS **5,250** CITATIONS

SEE PROFILE

# Infrared Investigation of Fluoride Occluded in Double Four-Member Rings in Zeolites

Luis A. Villaescusa<sup>†</sup>, Francisco M. Márquez, Claudio M. Zicovich-Wilson<sup>‡</sup>, and Miguel A. Camblor<sup>\*,§</sup>

*Instituto de Tecnología Química (U.P.V.-C.S.I.C.), Avda. los Naranjos s/n, 46022, Valencia, Spain*

*Received: August 17, 2001; In Final Form: November 5, 2001*

Three infrared absorption bands related to fluoride occluded within double four-member ring units of zeolites exist: one corresponds to fluoride itself and the other two are localized vibrations of the cage appearing at a different wavenumber depending on the presence or absence of fluoride within the cage. This is demonstrated by comparison of the vibrational spectra of a series of as-made and calcined octadecasil materials containing varying degrees of fluoride and aluminum and is further supported by *ab initio* quantum chemical calculations.

## Introduction

Zeolites present a large variety of different framework types that are among the most influential factors in determining their applications. However, solving a zeolite structure is frequently very challenging because of the difficulty in synthesizing crystals large enough for single-crystal diffraction studies. Important advances in crystallography have recently allowed the structural solution of complex zeolites such as VPI-9<sup>1</sup> or SSZ-23,<sup>2</sup> but it would be helpful to know beforehand of what kind of building blocks the zeolite is made. Vibrational spectroscopy could give this type of information if localized modes, assigned to specific units, would exist in this type of materials, an issue that is still controversial. We present here experimental evidence for the existence of localized modes assigned to a specific structural unit (the double four-member ring) in zeolites. We also show an absorption band caused by the vibration of fluoride anions inside that unit. Furthermore, these spectroscopical results are compared with *ab initio* calculations and interpreted in terms of the mutual perturbation between the fluoride and the cage motions.

Four-member rings (4MR) are units containing four  $\text{TO}_{4/2}$  tetrahedra (T being Si or Al) linked through oxygen bridges. These types of units are ubiquitous among zeolites that contain a large aluminum content.<sup>3</sup> However, they were considered to be highly unstable for pure silica compositions, where 5MR units are more frequent, until pure silica sodalite<sup>4</sup> and SSZ-24<sup>5</sup> (both plenty of 4MR and completely devoid of 5MR) were synthesized. But the idea still remained that double four-member ring units (D4R) would be too unstable for pure silica materials. Recently, octadecasil<sup>6</sup> and ITQ-7,<sup>7</sup> two pure silica phases containing D4R cages, have been synthesized. In both phases the as-made form contains fluoride anions occluded in the D4R cage.

## Materials and Methods

Octadecasil (framework code AST) can be synthesized in aqueous medium in the presence of fluoride anions and an adequate organic cation.<sup>6,8</sup> For the work presented here, we have

used *N,N,N*-trimethyl-*tert*-butylammonium (TMTBA) as the organic cation, because it can be completely removed, together with fluoride, by calcination,<sup>8</sup> and also because it allows the preparation of the material in a wide range of Si/Al ratios.<sup>9</sup> The organic cation fills the large octadecahedra cage from which this structure got its name. To counterbalance that positive charge the material may contain  $\text{F}^-$  or  $[\text{AlO}_4]^-$  tetrahedra in the framework, so its ideal chemical composition may be expressed as  $[(\text{C}_7\text{H}_{18}\text{N})_2\text{F}_{(2-x)}] \cdot [\text{Si}_{(20-x)}\text{Al}_x\text{O}_{40}]$ .<sup>9</sup> Fluoride resides inside the small D4R cages,<sup>6</sup> whereas Al substitutes for Si in the framework. When the Al content increases, the fluoride content decreases to keep electrical balance.<sup>9</sup> The octadecasil materials were synthesized hydrothermally using the previously reported procedure for pure silica AST with  $\text{F}^-$  as a mineralizer and TMTBA as a structure-directing agent.<sup>8</sup> The only modification with respect to the reported procedure for pure silica AST is that here varying amounts of aluminum were introduced into the crystallizing mixture. Al isopropoxide was dissolved in a solution of the hydroxide form of the structure-directing agent before the hydrolysis of the tetraethyl orthosilicate used as a source of  $\text{SiO}_2$ . The overall composition of the starting mixtures was  $\text{SiO}_2: x \text{ Al}_2\text{O}_3: (0.5 + 2x) \text{ N,N,N-trimethyl-}t\text{-butylammonium hydroxide [TMTBA(OH)]}: 0.5 \text{ HF}: 15 \text{ H}_2\text{O}$  with  $x = 0, 0.07, 0.13$ , and  $0.2$ . The crystallizations were performed in Teflon-lined stainless steel autoclaves under rotation (60 rpm) at 423 K. After selected times (6–15 days) the products (pH between 7.0 and 9.0) were filtered and the solids washed and dried overnight at 100 °C. Yields were between 14 and 18 g of zeolite per 100 g of gel.

Phase purity and crystallinity were determined by conventional powder X-ray diffraction (XRD) by using a Philips X'Pert diffractometer (Cu  $\text{K}\alpha$  radiation provided by a curved Cu monochromator). Fourier transform infrared (FT-IR) spectra in the region of framework vibrations ( $1900\text{--}300 \text{ cm}^{-1}$ ) were recorded on a Nicolet 710 FTIR spectrometer with use of the KBr pellet technique. FT-Raman spectra were recorded on a Bruker spectrometer, model RFS 100/s. The 1.064-nm line of a diode pumped Nd:YAG laser was used for excitation along with a high-sensitivity Germanium diode detector, cooled to liquid nitrogen temperature. The laser Raman spectra were examined in the  $180^\circ$  scattering configuration with a sample cup specially designed for this study. About 10 mg of each sample was pressed into the sample cup and then mounted on the sample holder. Various laser powers were tried so that the optimum power (130 mW) was selected. The sample temperature was controlled by measuring the Stokes/anti-Stokes

\* Corresponding author. E-mail: macambor@iqe.es.

<sup>†</sup> Current address: Departamento de Química, Universidad Politécnica de Valencia, Avda. los naranjos s/n, 46022-Valencia, Spain.

<sup>‡</sup> Current address: Departamento de Física, Universidad Autónoma del Estado de Morelos, Av. Universidad 1001, Col. Chamilpa, 62210 Cuernavaca (Morelos), Mexico.

<sup>§</sup> Current address: Industrias Químicas del Ebro, Polígono de Malpica, Calle D, no. 97, 50057 Zaragoza, Spain.

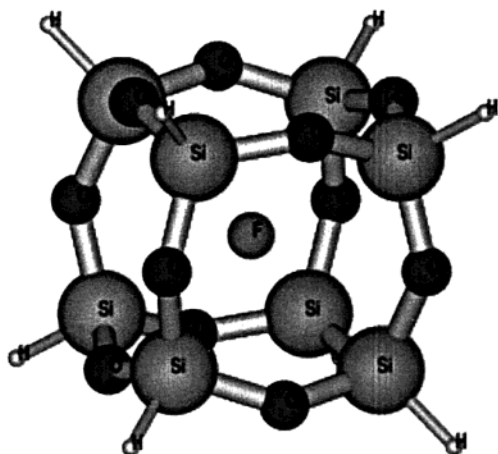


**Figure 1.** The CG-F cluster used in the quantum chemical calculations to study a zeolitic D4R unit with a fluoride anion occluded inside. The corresponding CG cluster, devoid of  $F^-$ , was also studied (not shown).

intensity ratio of Raman scattered radiation. The spectral resolution and reproducibility was experimentally determined to be better than  $4\text{ cm}^{-1}$ , and the number of scans varied from 700 to 3000 with recording times of 30 min to 2 h. The Raman spectra were corrected for instrumental response by using a white-light reference spectrum.

Ab initio calculations have been performed on cluster models that simulate a pure silica D4R unit both with and without  $F^-$ , which is labeled as CG-F and CG, respectively, in the following text. The zeolitic part of the system is represented by a molecular model consisting of eight Si atoms, placed at the corners of a cube and connected through O atoms. Accordingly, each Si is bonded to three O, and the remaining "dangling" bonds, that would connect the cage with the rest of the zeolitic structure, are saturated by H atoms (Figure 1). In CG-F the fluoride anion is located at the center of the cavity. Even though the D4R unit has tetragonal symmetry in the silica zeolites considered here; in the present theoretical calculations, the cubic symmetry,  $O_h$ , has been kept in all cases. The errors in the calculated vibrational modes possibly caused by the slight structural differences between the tetragonal and cubic CG models, are expected to be negligible with regard to other approximations assumed (border conditions of the cluster, basis set, Hamiltonian, etc.). On the other hand, a higher symmetry in the systems results in less expensive ab initio calculations and largely facilitates the analysis of the vibrational modes.

Calculations have been performed with the GAUSSIAN-94 code<sup>10</sup> at the density functional level of theory by using a 6-31G\* basis set.<sup>11</sup> The Becke 3<sup>12</sup> and the Perdew–Wang 91<sup>13</sup> functionals have been used for exchange and correlation, respectively. This level of theory has proved to be suitable for an accurate treatment of zeolitic compounds with a reasonable cost in terms of computational resources.<sup>14,15</sup> The total charge of model CG-F is  $-1\text{ e}$ , owing to the presence of the fluoride anion, whereas model CG is electrically neutral. All structures have been fully optimized under the above-mentioned symmetry constraint by using gradient techniques. The optimized SiO bond lengths are 1.642 and 1.629 Å, whereas the SiOSi bond angles are  $148.0^\circ$  and  $141.2^\circ$  for CG and CG-F, respectively. Concerning model CG, these values are in good agreement with previous theoretical calculations performed at a similar level of accuracy.<sup>16</sup> The corresponding force constant matrixes have been calculated analytically for the optimal geometries and then diagonalized to obtain the normal vibration modes and frequencies. The characterization of the modes have been performed

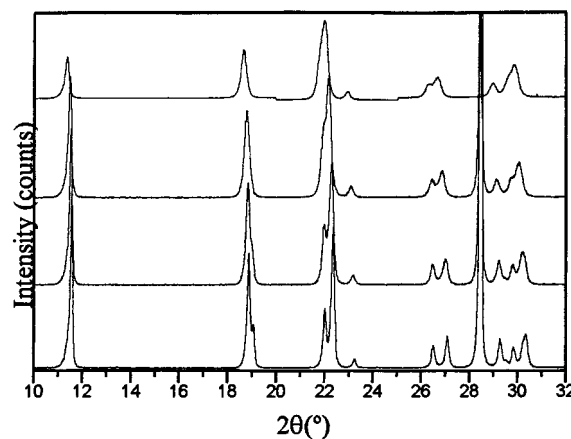


**Figure 2.** XRD patterns of as-made octadecasil materials with (from bottom to top) 0, 0.52, 1.18, and 1.54 Al per unit cell of 20 tetrahedra. The intense peak at  $28.44^\circ$  is from Si powder used as an internal standard.

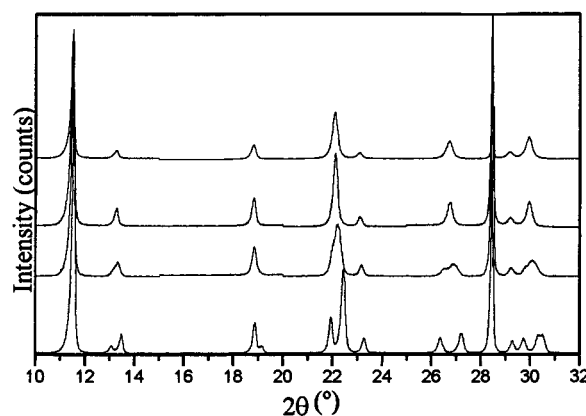


**Figure 3.** XRD patterns of calcined octadecasil materials with (from bottom to top) 0, 0.52, 1.18, and 1.54 Al per unit cell of 20 tetrahedra. The intense peak at  $28.44^\circ$  is from Si powder used as an internal standard.

with use of the symmetry and atomic component analysis implemented in the GAUSSIAN-94 program.<sup>10</sup> In both, CG and CG-F, all vibration frequencies are real, indicating the optimized structures are true energy minima.

## Results and Discussion

All the as-made and calcined samples are pure and highly crystalline AST materials (Figures 2 and 3). We found no signs of amorphous or crystalline impurities in the as-made materials by scanning electron microscopy, IR, and  $^{19}\text{F}$  or  $^{29}\text{Si}$  magic-angle spinning (MAS) NMR (see Supporting Information). In the calcined solids the intensity of selected XRD reflections is always within 90–100% of the pure silica sample (which fully retains its structural integrity after calcination, as demonstrated in ref 8). Indexing of the XRD patterns of the as-made and calcined materials with an internal standard showed a continuous increase in unit cell volume and a continuous decrease in the degree of tetragonal distortion as the amount of Al in the material increased. We interpret these results as a strong indication of a smooth and homogeneous distribution of Al within the samples. Direct evidence of the homogeneous distribution of Al has been additionally obtained by performing X-ray photoelectron spectroscopy analysis after different levels of sputtering with a fast  $\text{Ar}^+$  beam (see Supporting Information).

Figure 4 shows the IR spectra of several as-made octadecasil materials with varying aluminum contents. Interesting changes

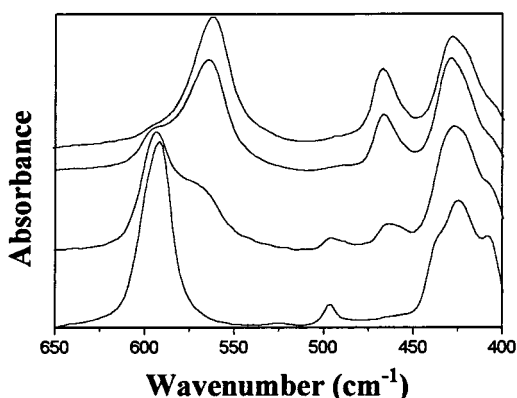


**Figure 4.** IR spectra of as-made octadecasil materials with the following unit cell contents (from bottom to top): 0.00 Al, 1.90 F; 0.56 Al, 1.27 F; 1.18 Al, 0.59 F; and 1.54 Al, 0.52 F. The spectra were normalized with respect to the intensity of the organic bands appearing at about 1400  $\text{cm}^{-1}$  (not shown). The organic content is constant for all the samples ( $2.00 \pm 0.03$  N per unit cell).

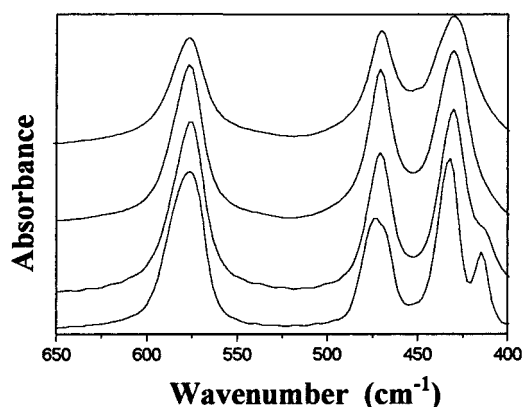


**Figure 5.** IR spectra of calcined octadecasil materials with the following unit cell contents (from bottom to top): 0.00 Al, 1.90 F; 0.56 Al, 1.27 F; 1.18 Al, 0.59 F; and 1.54 Al, 0.52 F.

occur in the 550–600  $\text{cm}^{-1}$  region of the infrared spectra of octadecasil as the Al content increases: a single band at 592  $\text{cm}^{-1}$  for the pure silica material decreases in intensity and a new one at 562  $\text{cm}^{-1}$  appears and increases in intensity as the Al content increases. The material with the highest Al and lower F content (1.54 Al and 0.52 F per unit cell of 20 tetrahedra) still shows a small shoulder at about 592  $\text{cm}^{-1}$ . By contrast, all the calcined materials show a single band at 576  $\text{cm}^{-1}$  (Figure 5).

Several authors have recently assigned bands in this region (575.8,<sup>17</sup> 560,<sup>18</sup> 550,<sup>19</sup> or 570<sup>20</sup>  $\text{cm}^{-1}$ ) to the vibration of the D4R unit in other zeolites. However, the assignation of vibrational bands to discrete structural units was criticized by others,<sup>21</sup> and the possibility to assign bands to the vibration of individual units within a framework still remained controversial.<sup>22</sup>

The appearance of a single band in this region for the pure silica whereas two bands appear in the aluminosilicate materials cannot be simply explained by a change in symmetry. The as-made samples are all tetragonal (with a decrease in the tetragonal distortion as the Al content increases), while, in the calcined materials only, for the two samples with higher Al content there is an apparent increase in symmetry to cubic (which is a likely result of disorder).<sup>8</sup> Thus, the possibility to assign these two bands to D4R units either with and without F<sup>−</sup> or with and without Al arises. After calcination there is a single band, suggesting the two bands in the as-made materials are not caused

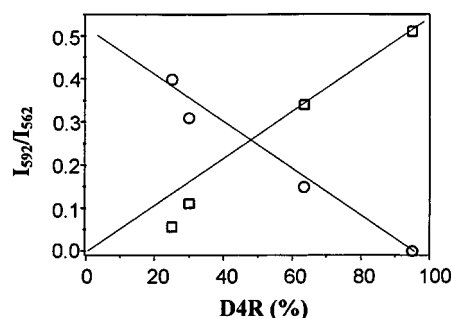


**Figure 6.** Correlation between the normalized intensities of the infrared bands at 592 and 562  $\text{cm}^{-1}$  in the IR spectra of octadecasils and the relative fraction of D4R cages with (□) or without (○) occluded F<sup>−</sup> (from chemical analysis and assuming all F<sup>−</sup> anions are occluded inside D4R cages).

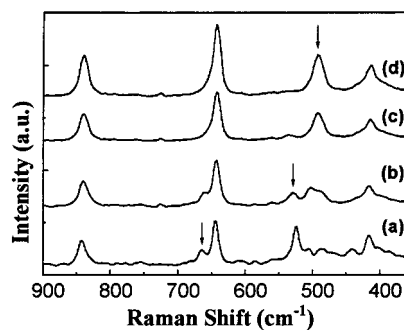


**Figure 7.** Near-IR-FT-Raman spectra of as-made octadecasil materials with the following unit cell contents: 0.00 Al (a); 0.56 Al, 1.27 F (b); 1.18 Al, 0.59 F (c); 1.54 Al, 0.52 F (d).

by D4R units with and without Al, respectively, because otherwise two bands would also be expected in the calcined materials. However, this cannot be regarded as strong evidence because it is unclear to what extent Al is removed from the framework at the high temperatures of the calcination (950 °C).<sup>9</sup>

The fact that the position of the bands is not affected by the Al content (within 2  $\text{cm}^{-1}$ ) suggests the vibration involves mostly the motion of oxygen atoms. Otherwise, a significant shift to lower wavenumbers should be expected upon increasing the Al content of the framework. This, rather than the appearance of new bands related to Al, is what usually occurs in zeolites upon isomorphous substitution of Si by Al. Then, it is the occlusion of F<sup>−</sup> inside the D4R unit what affects the motion of the oxygen atoms, making them vibrate at a different frequency than in the case of a void cage. As a matter of fact, an analysis of the structure of as-made octadecasil<sup>6</sup> reveals that the motion of the oxygen atoms in the F-[4<sup>6</sup>] unit must be highly constrained; the distance between opposite oxygens in the D4R unit is 5.38 Å. With van der Waals radii of 1.35 and 1.33 Å for O and F, respectively, this leaves little free space (barely 0.02 Å) and hence a restricted mobility for the O with a concomitant shift to larger wavenumbers in the spectrum. Figure 6 shows the correlation between the normalized intensities of the 592 and 562  $\text{cm}^{-1}$  bands and the relative occupancy of D4R by fluoride (according to chemical analysis and assuming all F is in D4R cages, as supported by <sup>19</sup>F MAS NMR, not shown).

Raman spectra of several as-made octadecasil materials with different Al and F contents are shown in Figure 7. In Figure 7a, the pure silica material possesses Raman bands at ca. 841, 664, 643, 524, 441, and 416  $\text{cm}^{-1}$ . As in IR spectroscopy, by decreasing the F<sup>−</sup> content (Figure 7b–d), several interesting changes can be observed. Thus, the bands observed at 664 and 524  $\text{cm}^{-1}$  in the pure silica material decrease in intensity, and



concomitantly, a new band at ca.  $491\text{ cm}^{-1}$  appears and increases in intensity as the  $\text{F}^-$  content decreases. The Raman recording of the calcined materials was unsuccessful showing a broad background at high frequency caused by sample heating effects.

The nature of the IR bands observed within the region at  $550\text{--}600\text{ cm}^{-1}$  has also been investigated by means of *ab initio* quantum chemical calculations. For this purpose, the normal vibration modes and frequencies of clusters CG-F and CG have been considered.

The calculated vibrational spectra in the  $550\text{--}600\text{ cm}^{-1}$  region show peaks at  $595$  and  $576\text{ cm}^{-1}$  for models CG-F and CG, respectively. The two modes associated with these frequencies have the same symmetry ( $A_{1g}$ ) and similar atomic composition in the zeolitic part. This strongly suggests that both correspond to the same structural motion, and the shift toward higher frequency values in the former mainly results from the perturbation caused by the occluded  $\text{F}^-$ . The modes correspond to a ring-opening vibration, as characterized in ref 16 for a tetragonal pure silica D4R unit, and the slight difference between the present result for CG and the frequency reported there ( $581\text{ cm}^{-1}$ ) can be attributed to the different point symmetry and Kohn–Sham Hamiltonian considered in each case. Other previous calculations of the same mode in cubic silasesquioxanes without  $\text{F}^-$ , but performed by a quite different methodology, i.e., the empirical classical force-field approximation, yields the same frequency value as in the present *ab initio* calculations for the CG model.<sup>23,24</sup>

These theoretical results are in full agreement with the previous assignment of the experimental bands in the same zone, as the modes in the CG-F and CG models do correspond to the bands featured by the as-made and calcined pure silica materials, respectively. The excellent correlation between theoretical and experimental results ( $595$  vs  $592\text{ cm}^{-1}$  and  $576$  vs  $576\text{ cm}^{-1}$ , in the as-made and calcined systems, respectively) does indicate that the small clusters used are enough to describe these vibration modes and supports the hypothesis that they are mainly localized into the D4R unit, in agreement with previous suggestions.<sup>24</sup>

It is also interesting to consider the region around  $470\text{ cm}^{-1}$ . In the as-made materials (Figure 4) a band at  $466\text{ cm}^{-1}$ , absent in the pure silica material, starts to show up and increases in intensity as the Al content increases (and  $\text{F}^-$  content decreases). In the calcined materials (Figure 5) a single band exists at about  $470\text{ cm}^{-1}$ . We also assign this band to the D4R unit devoid of the fluoride guest. No and co-workers calculated the normal modes of zeolite A and assigned bands at  $550$  and  $464\text{ cm}^{-1}$  to the vibration of the D4R unit, in good agreement with our experimental assignment.<sup>19</sup>

On the other hand, the fluoride anion itself must have its own vibration modes within the D4R cage. These vibrations can be expected to be much localized in character, because the long Si–F distance of  $2.66\text{ \AA}$ <sup>6</sup> indicates a rather weak interaction between Si and F. This interaction is also supported by the decrease of the cage size upon occlusion of F, as it arises from the optimized geometrical parameters of models CG and CG-F given above. In the spectrum of octadecasil a band exists at  $496\text{ cm}^{-1}$  (Figure 4) that cannot be assigned to the organic cation and whose intensity decreases as the fluoride content decreases. This band, which is also present in the spectrum of as-made octadecasil prepared by using a different organic cation (dimethylpiperidinium), disappears upon calcination. Under the assumption that the band at  $496\text{ cm}^{-1}$  in the as-made samples corresponds to a localized mode, the same mode is also expected

to appear within the same energy region in the calculated vibrational spectrum of cluster CG-F. Indeed, the calculated spectrum of CG-F displays three degenerated modes of  $T_{1u}$  symmetry at  $499\text{ cm}^{-1}$  that apparently shift to  $450\text{ cm}^{-1}$  in model CG. The former involve the motion of both the  $\text{F}^-$  and the zeolitic part of the clusters and could be attributed to the experimental band at  $496\text{ cm}^{-1}$ . Nevertheless, the fact that the corresponding mode in model CG is not present in the region around  $450\text{ cm}^{-1}$  of the spectrum of the calcined sample causes some doubts about this assignation. It is likely, therefore, that these localized modes either do not exist in the actual calcined and as-made zeolites or they shift to other frequency regions as result of the perturbation caused by the rest of the framework, not considered in the cluster models.

An alternative and more satisfactory interpretation of the band at  $496\text{ cm}^{-1}$  can be found in the as-made sample. In cluster CG-F the three additional modes resulting from the occlusion of  $\text{F}^-$  in the cage appear at  $122\text{ cm}^{-1}$ . The vibrational analysis indicates that such modes mainly involve the three translational degrees of freedom of the  $\text{F}^-$  ion ( $T_{1u}$  symmetry) with practically null components on the cage atoms. As mentioned above, the free space for the motion of the  $\text{F}^-$  ion within the cage should be very small. Under such extreme conditions of spatial confinement and in agreement with previous works,<sup>25,26</sup> the harmonic approximation used in the vibrational analysis of the GAUSSIAN code is not valid to describe the system, and the confined harmonic oscillator model should be used instead.

According to these previous findings,<sup>25,26</sup> the confinement effect results in a blue-shift of the IR absorption frequency that increases as the size of the cavity decreases. Comparing the calculated harmonic frequency and the experimental value, the shift of the  $\text{F}^-$  vibration frequency within the D4R cage can be estimated in about  $374\text{ cm}^{-1}$  which corresponds to a spherical free space with a  $0.24\text{-\AA}$  diameter (see eq 2.8 in ref 25). This value is significantly larger than the free space calculated from the crystal geometry and the van der Waals radii of  $\text{O}^{2-}$  and  $\text{F}^-$  ions ( $0.02\text{ \AA}$ ), because the SiO bond in a pure silica framework features a partial covalent character, and therefore, the electron density around the O atoms is smaller than in the purely ionic  $\text{O}^{2-}$ . The present results allow an indirect estimation of the effective van der Waals radius of O atoms in silicates of about  $1.24\text{ \AA}$ , if considering the crystallographic geometry of the D4R cage in pure silica octadecasil. As far as we know, this is the first quantitative estimation of this value in zeolites.

The latter assignation of the band at  $496\text{ cm}^{-1}$ , although involving a quite novel concept, i.e., the influence of the quantum spatial confinement on the vibrational frequency of a rather heavy atom such as  $\text{F}^-$ , is the most consistent with the spectroscopical data and with the fact that the fluoride anion closely matches the free space inside the D4R cage. This also highlights the need to consider the quantum confinement effects when interpreting vibrational spectroscopic experiments of species occluded in microporous materials.

In further support of the assignation above, we should now consider the case of ITQ-7 (framework code ISV). This is a new zeolite also containing D4R cages, and the cages are occupied by fluoride in the as-made samples.<sup>7,9</sup> As shown in Figure 8, the as-made material also presents a band at  $502\text{ cm}^{-1}$ , which disappears upon calcination and which we also assign to the vibration of the fluoride anion confined in the D4R cage. Although the  $550\text{--}600\text{ cm}^{-1}$  region ITQ-7 also presents bands that shift after calcination, the more complex structure of this

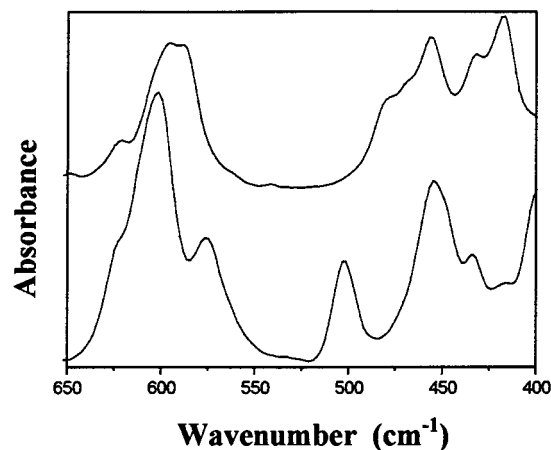


**Figure 8.** IR spectra of as-made (bottom) and calcined (top) pure silica ITQ-7.

zeolite compared with that of octadecasil makes a clear assignation more difficult.

**Acknowledgment.** Generous financial support by the Spanish CICYT (project MAT97-0723) is gratefully acknowledged.

**Supporting Information Available:**  $^{19}\text{F}$  and  $^{29}\text{Si}$  MAS NMR spectra and X-ray photoelectron spectroscopic analysis of as-made octadecasil. This material is available free of charge via the Internet at <http://pubs.acs.org>.

## References and Notes

- (1) McCusker, L. B.; Grosse-Kunstleve, R. W.; Baerlocher, Ch.; Yoshikawa, M.; Davis, M. E. *Microporous Mater.* **1996**, *6*, 295.
- (2) Cambor, M. A.; Díaz-Cabañas, M. J.; Perez-Pariente, J.; Teat, S. J.; Clegg, W.; Shannon, I. J.; Lightfoot, P.; Wright, P. A.; Morris, R. E. *Angew. Chem., Int. Ed. Engl.* **1998**, *37*, 212.
- (3) Baerlocher, C.; Meier, W. M.; Olson, D. H. *Atlas of Zeolite Framework Types*, 5th ed.; Elsevier: Amsterdam, 2001.
- (4) Bibby, D. M.; Dale, M. P. *Nature* **1985**, *317*, 157.
- (5) Bialek, R.; Meier, W. M.; Davis, M.; Annen, M. J. *Zeolites* **1991**, *11*, 438.
- (6) Caullet, P.; Guth, J. L.; Hazm, J.; Lamblin, J. M.; Gies, H. *Eur. J. Solid State Inorg. Chem.* **1991**, *28*, 345.
- (7) Villaescusa, L. A.; Barrett, P. A.; Cambor, M. A. *Angew. Chem., Int. Ed. Engl.* **1999**, *38*, 1997.
- (8) Villaescusa, L. A.; Barrett, P. A.; Cambor, M. A. *Chem. Mater.* **1998**, *12*, 3966.
- (9) Villaescusa, L. A. Ph.D. Thesis, Universidad Politécnica de Valencia, 1999.
- (10) Frisch, M. J.; Trucks, G. W.; Schlegel, H. B.; Gill, P. M. W.; Johnson, B. G.; Robb, M. A.; Cheeseman, J. R.; Keith, T.; Petersson, G. A.; Montgomery, J. A.; Raghavachari, K.; Al-Laham, M. A.; Zakrzewski, V. G.; Ortiz, J. V.; Foresman, J. B.; Cioslowski, J.; Stefanov, B. B.; Nanayakkara, A.; Challacombe, M.; Peng, C. Y.; Ayala, P. Y.; Chen, W.; Wong, M. W.; Andres, J. L.; Replogle, E. S.; Gomperts, R.; Martin, R. L.; Fox, D. J.; Binkley, J. S.; Defrees, D. J.; Baker, J.; Stewart, J. P.; Head-Gordon, M.; Gonzalez, C.; Pople, J. A. *Gaussian 94*, Revision E.1; Gaussian, Inc.: Pittsburgh, PA, 1995.
- (11) Hariharan, P. C.; Pople, J. A., *Chem. Phys. Lett.* **1972**, *16*, 217.
- (12) Becke, A. D. *J. Chem. Phys.* **1993**, *98*, 5648.
- (13) Perdew, J. P.; Wang, Y. *Phys. Rev. B* **1992**, *45*, 13244.
- (14) Boronat, M.; Zicovich-Wilson, C. M.; Viruela, P.; Corma, A. *Chem. Eur. J.* **2001**, *7*, 1295.
- (15) Boronat, M.; Viruela, P.; Corma, A. *J. Phys. Chem. B* **1998**, *102*, 9863.
- (16) Uzunova, E. L.; Nikolov, G. St. *J. Phys. Chem. B* **2000**, *104*, 7299.
- (17) Dutta, P. K.; Del Barco, B. *J. Phys. Chem.* **1988**, *92*, 354.
- (18) No, K. T.; Bae, D. H.; Jhon, M. S. *J. Phys. Chem.* **1986**, *90*, 1772.
- (19) No, K. T.; Seo, B. H.; Jhon, M. S. *Theor. Chim. Acta* **1989**, *75*, 307.
- (20) Iyer, K. A.; Singer, S. J. *J. Phys. Chem.* **1994**, *98*, 12679.
- (21) van Santen, R. A.; Vogel, D. L. *Adv. Solid-State Chem.* **1989**, *1*, 151.
- (22) de Man, A. J. M.; van Santen, R. A. *Zeolites* **1992**, *12*, 269.
- (23) Bärtsch, M.; Bornhauser, P.; Calzaferri, G.; Imhof, R. *J. Phys. Chem.* **1994**, *98*, 2817.
- (24) Marcolli, C.; Lainé, P.; Bühler, R.; Calzaferri, G.; Tomkinson, J. *J. Phys. Chem.* **1997**, *101*, 1171.
- (25) Zicovich-Wilson, C. M.; Planelles, J.; Jaskolski, W. *Int. J. Quantum Chem.* **1994**, *50*, 429.
- (26) Pazé, C.; Civalieri, B.; Bordiga, S.; Zecchina, A. *J. Phys. Chem. B* **1998**, *102*, 10753.